**한국ITS학회논문지**
제11권, 제1호 (2012년 2월)
pp.53~65

# UWB 차량통신 채널에서 IEEE 802.15.4a 시스템의 성능 분석

## Performance Analysis of IEEE 802.15.4a System in UWB Intra Vehicle Communications Channel

**골미라*** (Gulmira) **이 천 희**** (Cheon Hee Lee) **김 백 현***** (Baek Hyun Kim) **곽 경 섭****** (Kyung Sup Kwak)

### 요 약

최근 차량내 무선통신이 자동차 산업에서 큰 관심을 받고 있으며 UWB 기술이 차량내 통신 시스템에 유력한 기술로 고려되고 있다. 차량내 통신 채널의 측정과 모델링에 대한 많은 연구가 이루어져 왔으나, 차량내 통신환경에서 다양한 PHY Layer 기술에 대한 성능 분석은 여전히 많은 관심의 대상이 되고 있다. 본 논문의 목적은 차량내 채널환경에서 IEEE 802.15.4a PHY 시스템의 성능을 분석함에 있다. 새시와 엔진 부분의 채널 모델을 설정하고, 동기식 및 비동기식 수신기의 성능을 시뮬레이션을 통하여 분석하였다.

### Abstract

Recently wireless intra-vehicle communication has received a great interest from the automotive industry and ultra wideband (UWB) technology is considered as one of the potential candidate for this system. Many research works have been done on the measurement and modeling of intra-vehicle communication channel. However, very little work has been reported for the performance analysis of various PHY layer methods under the intra-vehicle communication environment. This paper is to study IEEE 802.15.4a standard in intra-vehicle channel and to evaluate its performance. Channel model in chassis and engine compartment is considered for evaluation. Through simulation BER performance of system with different receiver structures is analyzed.

**Key words** : UWB, IVC, Receiver, LR-WPAN, Channel model, bit error rate performance

† This research was supported by the National Research Foundation of Korea (NRF) grant funded by the Korea government(MEST)(No. No.2010-0016505).
* 주저자 : 인하대학교 정보통신공학부 석사과정
** 공저자 : 인하대학교 정보통신대학원 박사수료
*** 공저자 : 한국철도기술연구원, 공학박사
**** 공저자 및 교신저자 : 인하대학교 정보통신공학부 교수, 인하대학교 초광대역무선통신연구센터 센터장
† 논문접수일 : 2011년 9월 28일
† 논문심사일 : 2011년 12월 1일
† 게재확정일 : 2012년 1월 20일

# I. Introduction

Nowadays demands for wireless personal area networks (WPAN) are rapidly growing. One of them is automotive system which is the complex distributed computer system with various requirements on networking capabilities.

Modern car contains a lot of electronic devices, such as advanced safety systems, power train control, sensors, and many other diagnostic tools. There are several applications pushing the adoption of wireless communications in automotive systems, both in the intra-vehicle communications and in the inter-vehicle communications [1]. In this paper we focused on the wireless intra vehicle communications.

The great commercial potential of UWB systems for consumer and industrial applications has lead to a significant consideration of this system into automotive communications. UWB adopts narrow impulses to deliver message in high speeds within small areas. The extremely wide bandwidth of a UWB pulse makes it highly robust against narrow band interferences. The low power spectral density of UWB radio allows it to coexist with many other current wireless communication systems without harmful interference. And it is obvious that UWB is the best technology to resolve multipath of a communication signal reflected in the semi-closed metal environment like a car. In [2], the authors surveyed how manufacturers could achieve significant cost reduction through employing UWB wireless sensors instead of wired sensors.

There are two major types of UWB applications in vehicles. The first one is on-board high speed wireless intra vehicle communication (wireless HS-IVC), which are used to provide wireless Internet connectivity, video games, voice processing, car stereos, speakers and monitors for passengers. The second is wireless networked control systems (wireless NCS), which are suggested to replace the conventional wired controller area networks (CAN) that consists of number of sensors. Concept of intra vehicle communications system is shown in <Fig.1>. In a wireless NCS, electronic control units (ECU), associated sensors and actuators can be connected through wireless communication. In this paper, main contribution is on studying the performance of IEEE 802.15.4a system in IVC channel for wireless NCS.

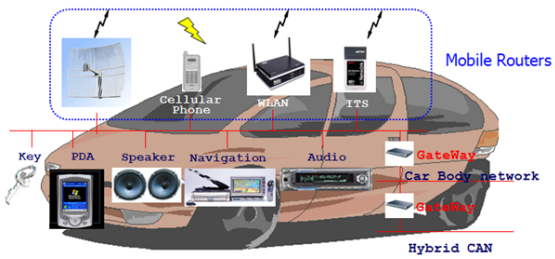


〈그림 1〉 IVC 시스템 개념도
〈Fig. 1〉 Concept of IVC system

The intra vehicle UWB channel measurements were performed for several scenarios, for example the fully occupied, empty passenger compartments, and small scale parameters have been defined in [3].

Channel modeling for military armored vehicle and outdoor propagation was conducted in [4]. Coverage area prediction for Multi-Band UWB system in IVC environment was derived in [5]. One more research work was dedicated for passenger compartment channel modeling and Time hopping BPSK (TH-BPSK) was analyzed under suggested channel model [6]. But selection of proper physical layer radio technology for wireless IVC system was not mentioned in the earlier studies.

In 2004, the IEEE established standardization group IEEE 802.15.4a [7] for LR-WPAN, that is one of the suitable candidates for realizing UWB sensor network for various applications including in-vehicle sensing.

Its key novelties are higher data rates, ranging capabilities, and more reduced energy consumption compared to other physical layer options. IEEE 802.15.4a defines various data rates from 110kbps up to 27.24Mbps, with the mandatory data rate of 0.851Mbps. The standard's compliant devices are capable of transmitting in at least one of three 500MHz wide bands centered at 499.2MHz, 4.493GHz, and 7.987GHz.

This paper is organized as follows. In section II, intra vehicle channel model and 802.15.4a standard including transmitter and receiver systems are analyzed. In section III, Simulation results are given and analyzed. Conclusion is given in Section IV.

# II. System model

## 1. Channel Model

UWB technology takes extremely wide transmission bandwidth, so it provides fine delay resolution in time domain, which results in the lack of significant multipath fading. Also, UWB signals demonstrate strong resistance to narrowband interference. These features make UWB promising technique for implementing the wireless NCS network.

We consider 2 types of channel model for sensor network in intra vehicle environment depending on its physical structure.

### 1) Channel model in engine compartment

The reason for modeling wireless channels in engine compartment is that some sensors like temperature detectors and oxygen sensors are located here and they transfer signal to ECU. Many auto components are placed in engine compartment so there are always some metallic obstacles between transmitter and receiver.

In engine compartment channel, paths arrive in clustering manner, so UWB channel can be represented by the classical S-V (Saleh Valenzuela) model [8]. The classical S-V channel impulse response to account for clustering of multipath components (MPC) in engine compartment of car is expressed as :

$$h(t) = \sum_{l=0}^{L} \sum_{k=0}^{K} \alpha_{k,l} \exp(j\theta_{k,l}) \delta(t - T_l - \tau_{k,l}) \qquad (1)$$

where $L$ is the number of clusters, $K$ is the number of MPCs within cluster, $\alpha_{k,l}$ is the multipath gain of the $k$-th path in the $l$-th cluster, that $T_l$ is the arrival time of the first path within the $l$-th cluster, assuming that the first path in the first cluster arrives at time zero, $\tau_{k,l}$is the delay of the $k$-th path within the $l$-th cluster, and $\theta_{k,l}$ is the phase shift of the $k$-th path within $l$-th cluster which takes values between 0 and π. Arrival of clusters and the arrival of the paths within a cluster are described as two Poisson processes [9]. Accordingly, the cluster interarrival time and the path interarrival time within a cluster are defined by exponential distribution, and are described as following functions:

$$\begin{aligned} p(T_l | T_{l-1}) &= \Lambda \exp[-\Lambda(T_l - T_{l-1})], \quad l > 0, \\ p(\tau_{k,l} | \tau_{(k-1),l}) &= \lambda \exp[-\lambda(\tau_{k,l} - \tau_{(k-1)l})], \quad k > 0, \end{aligned} \qquad (2)$$

where $\Lambda$ is the cluster arrival rate, and $\lambda$ is the path arrival rate in clusters.

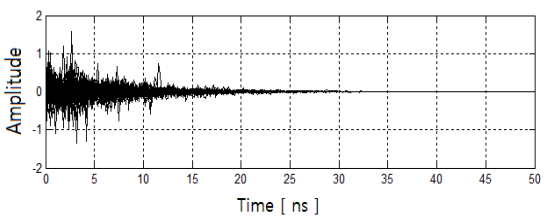


〈그림 2〉 엔진단의 채널 임펄스 응답
〈Fig. 2〉 Channel impulse response for engine compartment

Furthermore, S-V model assumes that the average power of both the clusters and the paths within the clusters decay exponentially as:

$$\overline{\alpha_{kl}^2} = \overline{\alpha_{00}^2} \exp\left(-\frac{T_l}{\Gamma}\right)\exp\left(-\frac{\tau_{kl}}{\gamma}\right) \quad (3)$$

where $\overline{\alpha_{00}^2}$ is the expected power of the first path in the first cluster, $\Gamma$ and $\gamma$ are the power decay constants for the clusters and paths within clusters. Root mean square delay spread is the standard deviation value of the delay of paths, weighted proportional to path power. It is defined as:

$$\tau_s = \sqrt{\frac{\sum_k (t_k - t_1 - \tau_m)^2 \alpha_k^2}{\sum_k \alpha_k^2}} \quad (4)$$

where $t_k$ and $t_1$ are the arrival time of the *k*-th path and the first path, respectively, $\alpha_k$ is the amplitude of the *k*-th path, and the mean excess delay $\tau_m$ is given as:

$$\tau_m = \frac{\sum_k (t_k - t_1)\alpha_k^2}{\sum_k \alpha_k^2} \quad (5)$$

Channel impulse response realization for engine compartment is shown in <Fig.2>.

〈표 1〉 엔진단의 채널 파라미터
〈Table 1〉 Channel parameters for engine compartment

| Channel parameters | Values in engine compartment |
|---|---|
| Mean RMS delay ($\tau_s$)[ns] | 1.5918 |
| Interpath arrival time ($1/\lambda$)[ns] | 0.2452 |
| Intercluster arrival time ($1/\Lambda$)[ns] | 3.0791 |
| Path amplitude | 11.0571 |
| Cluster amplitude | 5.19993 |
| Attenuation of first path ($\chi$) | 0.9452 |
| Path power decay factor ($\gamma$)[ns] | 1.084 |
| Cluster power decay factor ($\Gamma$)[ns] | 3.0978 |
| Path loss at 1m | 6.32 |
| Path loss coefficient. | 1.21 |

Depending on the statistical channel measurements, distribution of cluster and path amplitudes in intra vehicle environment are described as log-normal fading rather than Rayleigh fading. Probability density function of log normal distribution is given by:

$$f(x;\mu,\sigma) = \frac{\exp(-(\ln(x)-\mu)^2/2\sigma^2)}{x\sigma\sqrt{2\pi}}, \quad x \in [0,\infty) \quad (6)$$

Compared to UWB channel model defined in 802.15.3a standard for indoor and outdoor environment, in the intra-vehicle environment, the path or cluster arrival rates are greatly larger, while the path or cluster power decay constants are smaller. The reason for this phenomenon can be explained by two aspects. The propagation distance is relatively shorter, and the dense reflection caused by metallic objects in confined space. Therefore, the measurements of RMS are also less than those reported for the indoor UWB propagation.

From the observation of channel model in engine compartment, we can conclude that quasi metallic cavity characteristic of the intra- vehicle environments brings the dense and concentrated multipath.

### 2) Channel model in chassis

UWB propagation in this environment was specified because there are such sensors as wheel speed detectors that are installed at the wheel axes in modern vehicles. These sensors collect data and transfer to ECUs in front of a car.

In Chassis environment path clustering phenomenon was not observed so the channel impulse response [10] is represented as the sum of paths as:

$$h(t) = \sum_{k=0}^{K} \alpha_k \chi_k \exp(j\theta_k)\delta(t-\tau_k) \quad (7)$$

where K is the number of MPCs, $\alpha_k$ is the positive

random path gain, $\theta_k$ is the phase shift which considered to be uniformly distributed random variable in the range of [0, $2\pi$), $\tau_k$ is the path arrival time delays of the multipath components, and $\chi_k$ denotes distortion of the kth MPC. Impulse response realization for this channel is in <Fig.3>.

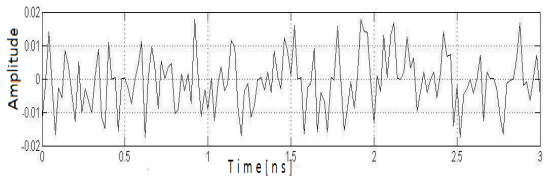


〈그림 3〉 섀시의 채널 임펄스 응답
〈Fig. 3〉Channel impulse response for chassis

The arrival of the paths is described as Poisson process, in which distribution of arrival intervals is given as:

$$p(\tau_k|\tau_{k-1}) = \lambda \exp[-\lambda(\tau_k - \tau_{k-1})], \quad k > 0 \tag{8}$$

For power delay profile (PDP) mean power of the paths are defined as:

$$E\{\alpha_k^2\} = \Omega \cdot \left(1 - \chi \cdot \exp\left(-\frac{\tau_k}{\gamma_{rise}}\right)\right) \cdot \exp\left(-\frac{\tau_k}{\gamma}\right) \tag{9}$$

Where $\gamma_{rise}$ determines how fast the PDP approaches to the maximum peak, $\gamma$ is the path decay factor, $\chi$ is the attenuation of the first path, and $\Omega$ is the integrated energy of the PDP.

〈표 2〉 섀시의 채널 파라미터
〈Table 2〉 Channel parameters for chassis

| Channel parameters | Value in chassis |
|---|---|
| mean RMS delay ($\tau_s$)[ns] | 0.4431 |
| Interpath arrival time ($1/\lambda$) [ns] | 0.4101 |
| Path amplitude | 6.5672 |
| attenuation of first path ($\chi$) | 0.924 |
| path power decay factor ($\gamma$) [ns] | 0.2141 |
| speed of PDP increases to peak | 0.2997 |

### 3) Path loss model

In the UWB IVC channel path loss is described by the ratio between transmitted power and received power. Path loss is normally formulated as:

$$PL(d) = PL_0 + 10 \cdot n \cdot \log_{10}\left(\frac{d}{d_0}\right) + S \tag{10}$$

where $PL_0$ is the path loss at the reference distance $d_0$ of 1m, $n$ is the path loss exponent, $d$ is the distance between the transmitting and the receiving antenna, and $S$ is a zero mean random variable which has Gaussian distribution. Equation (10) describes the path loss dependence on distance. In this paper, the frequency dependence of path loss is not considered.

In the IVC environment, transmit and receive antennas should be very close to each other (within the near field region) especially in engine compartment and beneath the chassis. In this situation common link budget is not valid because the behavior of the antennas is quite different from the behavior in the far field. So, link budget model proposed in [11] is applicable. This model considers an extra "near field loss" term in the far field loss, and the total loss of the link budget can be expressed as:

$$PL_{total}(r) = PL(d)\beta_{nf}(d) \tag{11}$$

where

$$PL(d) \propto \frac{1}{d^2} \tag{12}$$

and

$$\beta_{nf}(d) = 1 - e^{-\frac{d}{\tau_D}} \tag{13}$$

$PL_{total}$ is the total loss of the channel, $\beta_{nf}$ is correction factor due to near field effects, and $\tau_D$ is the distance decay constant, which depends on the physical dimensions of antenna.

## 2. IEEE 802.15.4a LR-WPAN standard

The IEEE 802.15.4a adopts UWB impulse radio to ensure robust data communications and in order to accommodate heterogeneous networks, it uses specific modulation, coding and ranging waveforms that can be detected well by both coherent and noncoherent receivers [12]. The following enhancements are introduced in this standard to satisfy the requirements for data communications :

- Extremely wide bandwidth characteristics that can provide very robust performance under harsh multipath and interference conditions;
- Concatenated forward error correction coding to provide flexible and robust performance;
- Optional UWB pulse control features to provide improved performance under some channel conditions while supporting reliable communications and precision ranging capabilities.

### 1) IEEE 802.15.4a Transmitter Structure

For the transmitter structure we follow the specification in the standard but without RS encoding block for simplicity. The corresponding block diagram of the transmitter is shown in <Fig.4>.

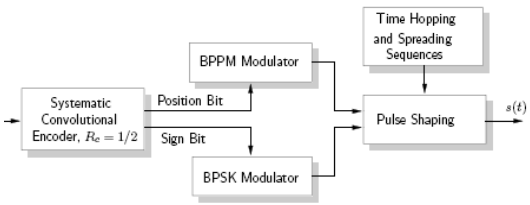


〈그림 4〉 IEEE 802.15.4a 송신기 블록다이어그램
〈Fig. 4〉 Block diagram of IEEE802.15.4a transmitter

For modulation, transmitter exploits BPPM/BPSK (Binary Pulse Position Modulation - Binary Phase Shift Modulation) hybrid modulation scheme.

After the channel coding, the systematic code bit is fed to a BPPM modulator and the non-systematic code bits is fed to a BPSK modulator. And the transmit signal [13] can be written as :

$$s(t) = \sum_{k=-\infty}^{\infty} (1-2a_k) p_k(t - kT_s - b_k T_{ppm}) \quad (14)$$

where $b_k \in \{0,1\}$ is the kth data symbol to be transmitted, that modulates position of the pulses in each symbol duration, $a_k \in \{0,1\}$ is a parity check bit associated with the kth data symbol, which is modulated onto the phase of the pulses, $T_s$ is the symbol duration, $T_{ppm} = T_s/2$ is PPM delay, and $p_k(t)$ is a burst of $N_{cpb}$ real valued chip pulses $w(t)$.

As in the standard, pulse train forms burst which is transmitted during symbol period. Burst signal is given by:

$$p_k(t) = \sum_{i=1}^{N_{cpb}} d_{i,k} w\left(t - iT_c - h_k T_{burst}\right) \quad (15)$$

where $T_c$ is the chip pulse duration that is usually 2ns, $T_{burst}$ is the burst hopping duration, which equals $T_{burst} = N_{cpb} T_c$, $N_{cpb}$ is the pulse number transmitted during 1 burst, and $d_{i,k} \in \{\pm 1\}$ denotes a time-varying binary spreading sequence. To facilitate multiple access, time hopping of bursts which is denoted as $h_k$ is enabled. For clear demonstration of transmission principle, <Fig.5> [14] sketches the data symbol structure for the mandatory data rate 0.85Mbps at the Mean PRF of 15.60 MHz.

The data symbols are $N_c$ chip periods long and divided into two BPPM intervals. To reduce the inter-symbol interference, the second half of each BPPM interval is left unused for guard interval. The active part of BPPM interval is subdivided into burst periods each composed of $N_{cpb}$ chip periods. Only one burst event is transmitted during the symbol period.

The burst position in the active portion of the BPPM interval is set by the TH ($h_k$) sequence.

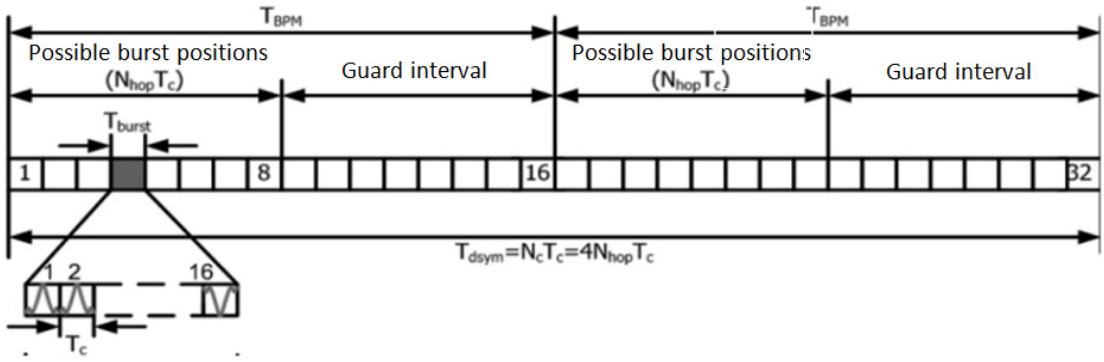


〈그림 5〉 0.85Mbps일 때 데이터 심벌 구조
〈Fig.5〉 Data symbol structure at the rate of 0.85Mbps

The modulation scheme enables a coherent receiver to receive 2 bits per transmit symbol, while it enables only one bit per symbol for noncoherent receivers. But for sensor networks, a more appropriate approach is to use the extra bits for coherent receivers to provide higher coding gain and improve the robustness. In order to ensure that the signals can still be decoded by noncoherent receivers, a systematic code has to be used. Convolutional encoder implemented in the IEEE 802.15.4a standard
has the rate of $R=1/2$ and with following generator functions:

$$g_0=[010],\ \ g_1=[101] \tag{16}$$

Convolutional encoder with a systematic and parity outputs specified in the standard is shown in <Fig.6>.

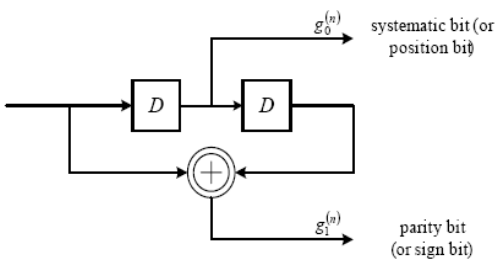


<그림 6> IEEE 802.15.4a 의 콘볼루션 인코더
〈Fig. 6〉 Convolutional encoder for IEEE802.15.4a

### 2) IEEE 802.15.4a Receiver Structure

Due to the use of systematic codes and mapping of the systematic code bit to BPPM as described above, both coherent and noncoherent reception of data are possible. Coherent reception assumes that reliable channel estimation is available at the receiver [15], whereas in the case of noncoherent reception no channel estimation is needed [16]. In the following part we present the suitable receiver structures for both reception modes.

*a) Coherent reception:*

In this paper we implement rake receiver which consists of bank of correlators also called fingers and detector for multipath environment.

Pulse modulation systems can take advantage of multi-path propagation by combining a large number of different and independent replicas of the same transmitted pulse. We assume the rake receiver for th coherent reception that is shown in <Fig.7>. A Rake receiver consists of bank of correlators also called fingers, and detector. In order to enable symbol rate sampling, the received signal can be correlated with a symbol-length template signal $m(t)$. Each rake finger is matched to a particular multipath component to combine the received multipath coherently If the receiver uses all

the L received paths, it is called all rake (ARake). In practical system implementation of ARake receiver is complex, therefore receivers with limited number of fingers as partial rake (PRake) and selective rake (SRake) receivers are applicable.

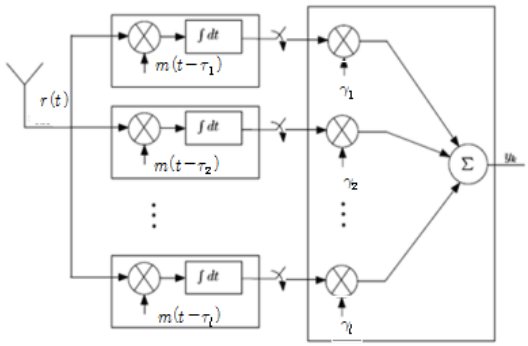


〈그림 7〉 TH-IR 시스템의 레이크 리시버 구조
〈Fig. 7〉 A Rake receiver structure for TH-IR system

In this paper, optimal receiver depicted in <Fig. 8> is implemented for simulation [17].

We note that ISI is negligible, because RMS delay spread values measured in two channel environment are much lower than symbol period.

Assuming that $s(t)$ in (14) is transmitted; the received signal is given by:

$$r(t) = s(t) * h(t) + n(t)$$

$$r(t) = \sqrt{E_p} \sum_{j=1}^{N_{cpb}} d_{i,k}(1-2a_k) p_k(t - jT_c - h_k T_{burst} - b_k T_{ppm}) * h(t) + n(t) \quad (17)$$

where *n(t)* is a zero mean, additive Gaussian noise, $h(t)$ is channel impulse response. And we drop the index k assuming that single user signal is received.

For simplicity, we use function $g(t) = p(t) * h(t)$.

And after despreading and denotation:

$$r(t) = \sqrt{E_p} \sum_{j=1}^{N_{cpb}} (1-2a_k) g(t - jT_c - h_k T_{burst} - b_k T_{ppm}) + n(t) \quad (18)$$

Transmitted energy has unit energy and it is:

$$E_g = \int_0^{T_g} g^2(t)dt, \leq 1$$

In optimal receiver, the correlation template is more complex and it is given by:

$$m(t) = \frac{1}{\sqrt{N_{cbp}}} \sum_{j=1}^{N_{cpb}} [p_0(t - jT_c - h_k T_{burst}) + p_0(t - jT_c - h_k T_{burst} - T_{ppm})] \quad (19)$$

For the IEEE 802.15.4a standard, receiver correlation template is different from the conventional PPM modulation because the received signal is modulated by PPM with BPSK and the exact positions of pulses cannot be obtained. The mathematical operation of cross correlator is to integrate the received signal with a correlation template over the interval of one symbol [18].

$$Z_{i,l} = \int_{-\infty}^{\infty} r(t)m(t-\tau_l)dt \,, i \in 0,1 \quad l = 0,1,\ldots,L-1 \quad (20)$$

Before evaluating the $Z_{i,l}$ we define the cross-correlation function $\alpha(\tau)$ between $g(t)$ and $p_0(t)$ as :

$$\alpha(\tau) = \int_{-\infty}^{\infty} g(t)p(t-\tau)dt \quad (21)$$

now we can obtain $Z_{0,l}$ as:

$$Z_{0,l} = \sqrt{E_p N_{cpb} E_g} \int_{-\infty}^{\infty} g(t)p_0(t-\tau_l)dt + \int_{-\infty}^{\infty} n(t)m(t-\tau)dt = = \sqrt{E_p N_{cpb} E_g}[\alpha(\tau_l) + \beta(\tau_l)] + \eta_{0,l}$$

similarly for $Z_{1,l}$:

$$Z_{1,l} = \sqrt{E_p N_{cpb} E_g} \int_{-\infty}^{\infty} g(t)p_0(t-\tau_l)dt + \int_{-\infty}^{\infty} n(t)m(t-\tau)dt = = \sqrt{E_p N_{cpb} E_g}[\alpha(\tau_l + T_{ppm}) + \beta(\tau_l)] + \eta_{1,l} \quad (22)$$

where $\beta(\tau_l)=\int_{-\infty}^{\infty} g(t-T_{ppm})p_0(t-\tau_l)dt$ and

$$\eta_{i,l}=\int_{-\infty}^{\infty} n(t)m(t-\tau_l).$$

The output of correlator is given to the combiner for defining decision variable $Z_i$ . Maximal ratio combining is one of the possible combining methods. In MRC, the output of each branch is multiplied by weighting factors $\{\gamma_{1,},.....,\gamma_L\}$, which is proportional to the signal amplitude on that branch. The decision variable $Z_i$ at the output of combiner can be expressed as:

$$Z_i=\sum_{l=1}^{L}\gamma_{l_l}Z_{i,l} \qquad i=0,1 \tag{23}$$

As an input for the detection of convolutional coding, the viterbi decoder gets the sequence of bits obtained by both position and phase modulated bits.

Position modulated bits are defined by the comparison of absolute values as:

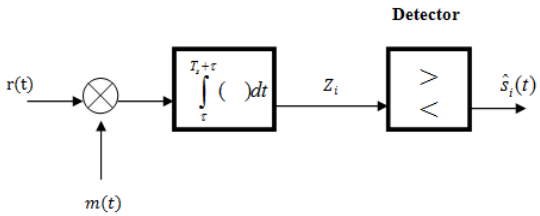


〈그림 8〉 BPPM/BPSK 방식에 등가적인 레이크 리시버
〈Fig. 8〉 Equivalent Rake receiver for BPPM/BPSK scheme

$$\hat{b_i}=\begin{cases}0, & \text{if} \quad |Z_0|>|Z_1| \\ 1, & \text{if} \quad |Z_0|<|Z_1|\end{cases} \tag{24}$$

Since the transmitted signal is phase modulated also, the phase modulated bits are defined as:

$$\hat{a_i}=\begin{cases}0, & \text{if} \quad |Z_i|<0 \\ 1, & \text{if} \quad |Z_i|>0\end{cases} \tag{25}$$

*b) Non-Coherent reception:*

Energy detection scheme is a popular receiver scheme used in UWB LR-WPAN systems. This non coherent receiver for Impulse-Radio UWB systems measures the energy in the two PPM signaling intervals [19]. Energy detection receivers are attractive for their limited complexity and low power requirements.

Conventional energy detection receivers consist of BPF, square low device, an integrator, and a sampling device. In this way the output at the energy detector is the samples of the energy gathered in the band of interest during the integration or sampling time. The energy detection receiver implemented for performance evaluation is shown in <Fig.9>.

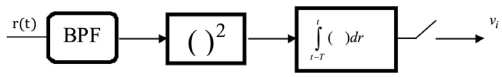


〈그림 9〉 BPPM/BPSK의 에너지 검출 수신기
〈Fig. 9〉 Energy detection receiver for BPPM/BPSK

The received signal is given by (17). It can be seen from equation that pulse burst is transmitted in first half or second half of the symbol depending on whether $b_k$ equals 0 or 1. The received signal in energy detection receiver passes through BPF for noise reduction.

Assuming that BPF does not cause distortion to the received signal, the optimum decision strategy to detect PPM modulated bits requires computing the energies as :

$$v_0=\int_0^{T_s}|r(t)|^2dt \tag{29}$$

$$v_1=\int_{T_{s/2}}^{T_{s/2}+T_h}|r(t)|^2dt \tag{30}$$

where $T_h$ is the duration of channel impulse response $h(t)$. In practice, $T_h$ is not known and takes different values depending on the channel

impulse response. Value of $T_h$ can be found that minimizes the bit error rate.

And the decision rule is given:

$$\hat{b}_i = \begin{cases} 0, \text{ if } & v_0 \geq v_1 \\ 1, \text{ if } & v_0 < v_1 \end{cases} \quad (31)$$

Using energy detection scheme only BPPM signal part is retrieved.

## III. Simulation Results

In this section, the simulation results are analyzed.

<Fig.10> presents the BER performance of different receivers in engine compartment channel. Results demonstrate that All Rake receiver with convolutional coding has better performance in case of high SNR. But for lower SNR case All Rake receiver with convolutional coding and without coding shows almost same result. It confirms that energy detection receiver has significantly poor performance compare to the rake receiver.

〈표 3〉 시뮬레이션 파라미터
〈Table 3〉 Simulation parameters

| Parameters | Value |
|---|---|
| Modulation<br>Coding | BPPM/BPSK<br>Convolutional Coding |
| #Burst positions per symbol Nburst | 32 |
| #Hop bursts Nhop | 8 |
| #Chips per Burst Ncpb | 2 |
| # Chips per symbol | 64 |
| Burst duration Tburst | 4ns |
| Symbol duration | 128ns |
| Data Rate | 7.8Mbps |

In <Fig.11>, the performance of SRake and PRake receiver with different number of fingers with MRC combining is shown. Depending on the channel characteristic, SRake and PRake with same number of fingers have identical performance.

In <Fig.12> the performance evaluation has been demonstrated for the chassis environment. As mentioned before, channel in chassis environment is expressed as multipath channel, where paths do not arrive in cluster form.

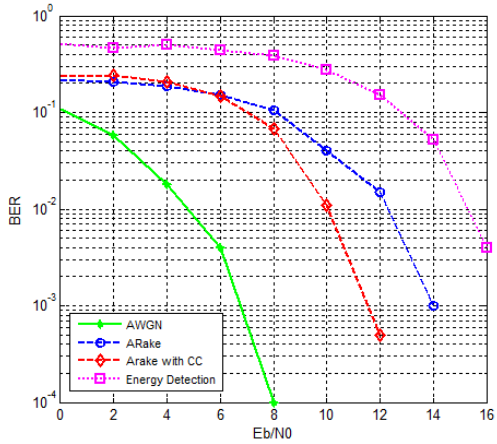


〈그림 10〉 엔진단에서 리시버들의 BER 성능
〈Fig. 10〉 BER performance for different receivers in Engine Compartment

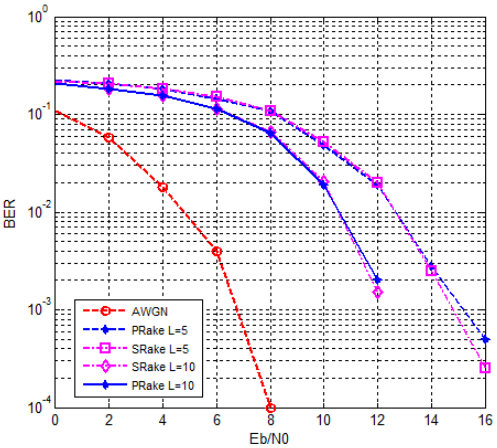


〈그림 11〉 엔진단에서 리시버의 finger 개수에 따른 BER 성능
〈Fig. 11〉 BER performance for receivers with different number of fingers in engine compartment

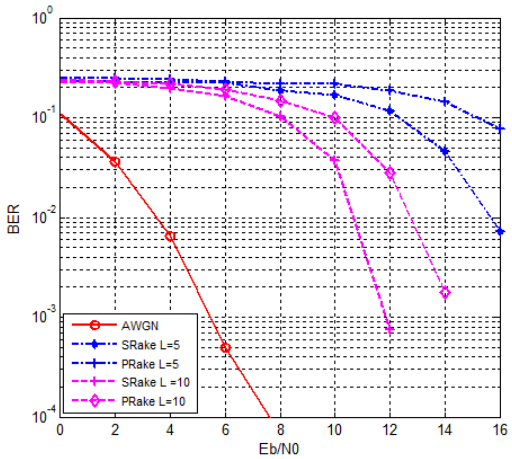


〈그림 12〉 섀시의 리시버들의 BER 성능
〈Fig. 12〉 BER performance for different receivers in chassis

using 10 fingers of SRake, while PRake requires $Eb/N0 = 14dB$ for reaching the same BER.

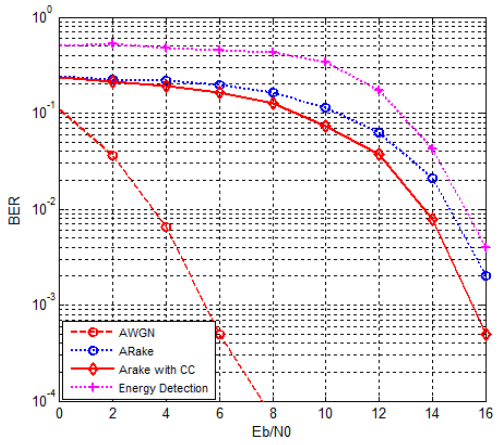


〈그림 13〉 섀시의 리시버의 finger 개수에 따른 BER 성능
〈Fig. 13〉 BER performance for receivers with different number of fingers in chassis

As shown in <Fig.13>, the result demonstrate a significant performance improvement using SRake as compared to PRake. From the results, it is possible to achieve a BER of $10^{-2}$ with $Eb/N0 = 11dB$

## IV. Conclusion

In this paper, we present the performance of IEEE 802.15.4a UWB LR-WPAN system for two types of intra vehicle channel environment as inside engine compartment and beneath the chassis.

We use new correlation template for Rake receiver. The simulation results show that Rake receiver outperforms conventional energy detection receivers for both channels.

For the engine compartment channel, SRake and PRake with the same number of fingers shows similar performance.

In the future work, interference effects from WLAN or Bluetooth will be analyzed and the mitigation method will be studied.

## References

[1] T. Nolte, H. Hansson and L. L. Bello, "Automative Communications-Past, Current and Future," *Proc. Emerging Technologies and Factory Automation conf,* pp.958-992 September 2005.

[2] J. Li and T. Talty, "Channel characterization for Ultra Wideband Intra Vehicle sensor networks," *Proc.Military Commun.Conf. (MILCOM),* pp.1-5, October 2006.

[3] L. Liu, Y. Wang, N. Zhang and Y. Zhang, "UWB channel measurement and modeling for the intra vehicle environments," *Proc. IEEE Int. Conf. Commun.Tech. (ICCT)*, pp. 381-384, Nov. 2010.

[4] P. C.Richardson, W. Xiang and W. Stark "Modeling of Ultra Wideband Channels within Vehicles," *IEE Journal on Selected areas in Comm.* vol. 21, no. 4, pp.906-912, April 2006.

[5] R. Kaneko, A. Yamakita and F. Maehara, "Coverage area prediction method of extremely

reliable in-car MB-OFDM communication," *Proc. IEEE Vehicular Technology Conf.(VTC),* pp.1-5, May 2010.

[6] W. Aldeeb, W. Xiang and P. Richardson, "A Study on the Channel and BER-SNR Performance of Ultra Wide Band Systems Applied in Commercial Vehicles," *Proc. IEEE Sarnoff Symposium,* pp.1-5, May 2007.

[7] IEEE 802.15 working group for WPANs, "Part 15.4: Wireless Medium Access Control (MAC) and Physical Layer (PHY) Specifications for Low-Rate Wireless Personal Area Networks (WPANs); Amendment 1: Add Alternated PHYs" March 2007.

[8] D.Cassioli, W.Ciccognani and A.Durantini "D 3.1-UWB Channel Model Report," *Tech.Rep. ISS-2001-35189-ULTRAWAVES*, November 2003.

[9] W. Niu, J. Li and T. Talty, "Ultra-Wideband Channel Modelling for Intra vehicle Environment," *Eurasip Journal on Wireless Communications and Networking* , vol. 2009. January 2009.

[10] A. F. Molisch, D. Cassioli and C. Chin "Comprehensive Standardized Model for UWB propagation channels," *IEEE Transactions on Antennas and Propagation,* vol. 54, no. 11, pp.3151-3166, November 2006.

[11] Z. Irahhauten, J. Dacuna, G. J. M. Janssen and H. Nikookar, "A link budget model for UWB-WPAN Applications," *Proc. European Conf. on Wireless Technology*, pp.95-98, September 2006.

[12] J. Zhang, P. V .Orli, Z. Sahinoglu, A. F. Molish and P. Kinney, "UWB Systems for Wireless Sensor Networks," in *Proc. of IEEE*, issue 2, pp.313-331, February 2009.

[13] Z. Ahmadian and L. Lampe, "Performance Analysis of the IEEE 802.15.4a UWB System," *IEEE Transactions on Communications*, vol. 57, no. 5, pp.1474-1485, May 2009.

[14] P.Median, J.R.Gallardo, J.Sanchez and F.Ramirez - Mireles, "Impact of Delay Spread on IEEE 802.15.4a Networks with Energy Detection Receivers," *Journal of Apllied Science and Technology*, vol. 8, no.3, pp.352-364, December 2010.

[15] V. Lottici and A. D'Andrea and U. Mengali, "Channel Estimation for Ultra-Wideband Communications," *IEEE Journal on Selected Areans in Communications*, vol. 20, no. 9, pp.1638-1645, December 2002.

[16] F. Wang, Z. Tian and B. M. Sadler, "Weighted Energy Detection for Noncoherent Ultra-Wideband Receiver Design," *IEEE Transactions on Wireless Communications,* vol. 10, no. 2, February 2011.

[17] M. D. Benedetto and G. Giancola, "Understanding ultra-wide band radio fundamentals" *New Jersey, Prentice Hall Professional Technical Reference*, 2003.

[18] J. D. Choi and W. E. Stark. "Performance of UWB with suboptimal receivers in multipath channels," *IEEE Journals on Selected Areas in Communications*, vol. 20, no. 9, pp.1754-1766, December 2002.

[19] E. Reyna, A. A. D'Amico and U. Mengali, "UWB Energy Detection Receivers with Partial Channel Knowledge," *Proc. on IEEE Int. Conf. ICC'2006 on Communications*, pp.4688-4693, June 2006.

## 저자소개


**골미라 (Gulmira Khuandaga)**

2009년 9월 ~ 현 재 : 인하대학교 정보통신공학부 석사과정
2006년 6월 : Mongolian University of Science and Technology, B.S

**이 천 희 (Lee, Cheon Hee)**

2002년 3월 ~ 현 재 : 인하대학교 정보통신대학원 박사수료
1996년 1월 ~ 현 재 : (주)에이스안테나 연구위원
1996년 2월 : 한남대학교 전자공학과(공학석사)
1994년 2월 : 한남대학교 정보통신공학과(공학사)

**김 백 현 (Kim, Baek Hyun)**

2003년 3월 ~ 현 재 : 한국철도기술연구원 신교통연구본부 선임연구원
2003년 2월 : 인하대학교 전자공학과 공학박사(전자통신전공)
1996년 2월 : 인하대학교 전자공학과 공학석사(전자통신전공)
1994년 2월 : 인하대학교 전자공학과 공학사 졸업

**곽경섭 (Kwak, Kyung Sup)**

2000년 3월 ~ 현 재 : 인하대학교 정보통신공학부 석좌교수(IFP)
2003년 8월 ~ 현 재 : 인하대학교 초광대역무선통신 연구센터(UWB-ITRC) 센터장
2009년 1월 ~ 2009년 12월 : 한국ITS학회 회장
2006년 1월 ~ 2006년 12월 : 한국통신학회 회장
2000년 3월 ~ 2002년 2월 : 인하대학교 정보통신대학원 원장
1989년 2월 ~ 1990년 3월 : 미국 IBM Network Analysis Center 연구원
1988년 2월 ~ 1989년 2월 : 미국 Hughes Network System 연구원
1988년 2월 : 미국 UCSD 통신이론 및 시스템 박사 졸업
1981년 12월 : 미국 USC 전기공학과 석사 졸업
1977년 2월 : 인하대학교 전기공학과 학사 졸업